3-12-2012

Accurate Spectral Measurements and Color Infrared Imagery of Excised Leaves Exhibiting Gaussian Curvature from Healthy and Stressed Plants

Christopher R. Little

Kenneth R. Summy
The University of Texas Rio Grande Valley

Recommended Citation

Little, C. R., & Summy, K. R. (2012). Accurate Spectral Measurements and Color Infrared Imagery of Excised Leaves Exhibiting Gaussian Curvature from Healthy and Stressed Plants. In (Ed.), Advanced Image Acquisition, Processing Techniques and Applications. IntechOpen. https://doi.org/10.5772/37300

7

Accurate Spectral Measurements and Color Infrared Imagery of Excised Leaves Exhibiting Gaussian Curvature from Healthy and Stressed Plants

Christopher R. Little[1] and Kenneth R. Summy[2]
[1]*Kansas State University*
[2]*The University of Texas - Pan American*
USA

1. Introduction

The interactions of light with a leaf are determined by the three-dimensional internal and external leaf structure as well as photosynthetic pigment content within the cells (Gamon and Surfus, 1999). The three-dimensional structure and pigment content of a leaf is determined by a number of factors including plant species and varieties within species (genetics), leaf age, and growth conditions including abiotic and biotic stress factors, hormonal activity, and light history (Gamon and Surfus, 1999; Nath et al., 2003). Stresses such as water loss, suboptimal temperatures, high soil salinity, disease, arthropod feeding damage, nutrient deficiency, chemical pollution, and micronutrient toxicities may alter the internal structure of leaves (Gausman, 1985).

During the past fifty years, remote sensing applications in agriculture have proven their effectiveness as non-destructive, rapid, and relatively inexpensive techniques for obtaining information about plants and crop status (Johannsen et al., 1999). Successful use of remote sensing in agriculture has been predicated on knowledge regarding the nature of electromagnetic radiation (EMR) and its interactions with vegetation. EMR is characterized by both electrical and magnetic properties and by both particles and waves, which are most commonly measured in micrometers (μm) or nanometers (nm). The totality of EMR emitted by the sun forms the electromagnetic spectrum, which extends from short-wavelength high-energy gamma and x-rays (< 300 nm) to long-wavelength low-energy microwaves and radio waves (> 1 mm) (Figure 1). Reflected EMR of greatest value in remote sensing of vegetation includes the visible spectrum (400 to 700 nm), which constitutes the basis for conventional photography, and the near- and mid-infrared regions (700 to 3,000 nm), which are not detectable by the human visual system. Extensive reviews of the theory and use of color-infrared (CIR) imagery to detect visible and invisible wavebands are provided in Avery and Berlin (1992), Campbell (2002), Jensen (2004, 2006), Lillesand et al. (2007), and Wilke and Finn (1996).

It has long been known that the degree to which incident EMR is absorbed, transmitted, or reflected by vegetation is governed by the presence of phototsynthetic pigments

(chlorophyll *a*, *b*; carotenes; xanthophylls; phaeophytin *a*, *b*) and the structure of cells within the spongy mesophyll layer of leaves (Gates et al., 1965; Gausman et al., 1969; Myers, 1970). A typical "spectral profile" of healthy foliage usually indicates a relatively low reflectance of blue and red wavelengths (400 to 500 nm and 600 to 700 nm, respectively), a slight increase in reflectance of green wavelengths (500 to 600 nm), and a substantial increase in reflectance of near-infrared (700 to 1,300 nm) and mid-infrared (1,300 to 3,000 nm) wavelengths (Figure 1). Reflectance of blue and red wavelengths (both of which are used to drive photosynthesis) is largely an effect of chlorophyll absorption, while reflectance of near-infrared (NIR) wavelengths is largely determined by the configuration and condition of air spaces within the spongy mesophyll layer of leaves (Lillesand et al., 2007). Water content of leaves appears to be the principal determinant of mid-infrared (MIR) reflectance. EMR in the green region of the spectrum is not absorbed to any extent by most plant species and is thus transmitted or reflected in relatively large quantities, hence the slight increase in reflectance of EMR near the center portion of the visible spectrum (Figure 1).

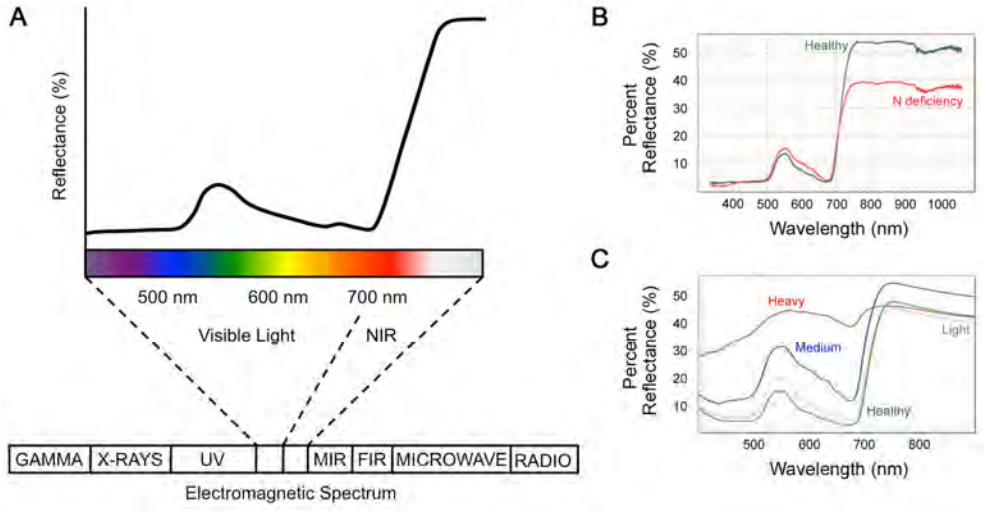

Fig. 1. The electromagnetic spectrum and a typical spectral reflectance curve for healthy plant tissues (A). Spectral reflectance curves for foliage of healthy and nitrogen deficient cucumber (*Cucumis sativus*) plants (B). Spectral reflectance curves for healthy foliage of *C. sativus* plants and those with "light", "medium", and "heavy" feeding damage by carmine spider mites (*Tetranychus cinnabarinus*) (C). Figure adapted from Summy et al. (2003) (A, B,) and Summy et al. (2007) (C), respectively.

Physiological stress in plants is commonly characterized by significant changes in reflectance of EMR in one or more regions of the spectrum. In subtle forms of stress in which leaf structure or water content has been altered without adversely affecting photosynthesis, changes in reflectance may be restricted to wavelengths in the NIR and/or MIR regions, neither of which is detectable by the human eye (Figure 2). Senescence, nutrient stress, pathogens, and insect predation have been shown to result in significant reductions of NIR reflectance by affected foliage (Wiegand et al., 1972; Murtha, 1978). In more advanced or

severe forms of stress in which absorption by photosynthetic pigments has been seriously impeded or halted, increases in reflectance of photosynthetically active EMR (blue and red wavelengths) are inevitable and are responsible for many of the visible symptoms of plant stress, e.g., *chlorosis*. This classic symptom of plant stress occurs when reflectance of red wavelengths increases to levels equivalent to those of green wavelengths and is perceived by the human visual system as yellow.

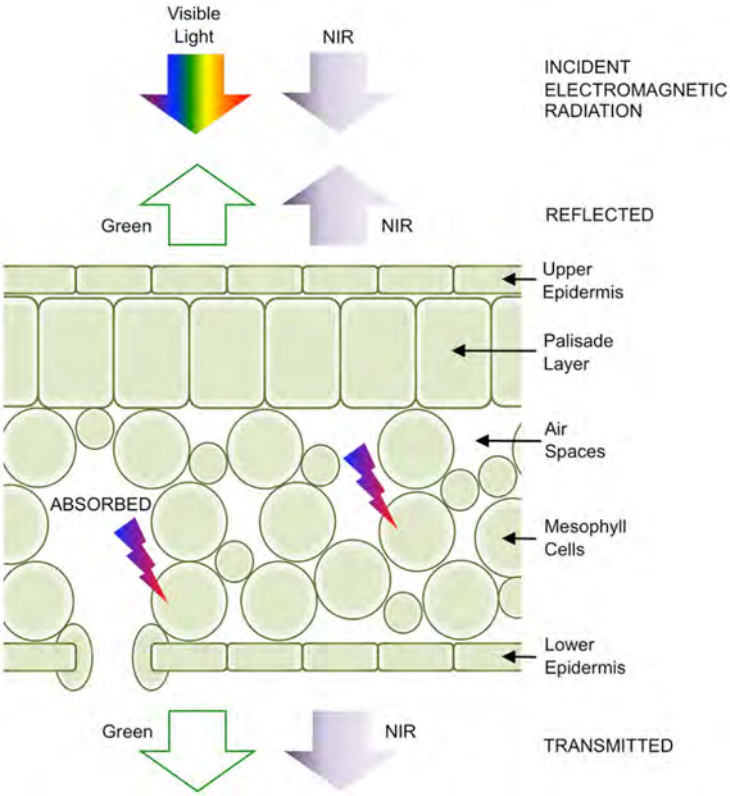

Fig. 2. Structure of a typical plant leaf showing patterns of transmission (green and NIR), absorption (blue and red), and reflectance (green and NIR) of incident electromagnetic radiation in various regions of the spectrum.

Use of remote sensing technology for detection and monitoring of plant stress caused by diseases and other factors has traditionally involved one or both of the following approaches: 1) *in situ* collection of spectral measurements using field spectroradiometers at ground level, and/or 2) acquisition of various types of imagery using sensors (e.g., cameras or scanners) mounted in aircraft or satellite platforms (see reviews in Avery and Berlin, 1992; Jensen, 2006; Lillesand et al., 2007; Cracknell and Hayes, 2007). This manner of data acquisition is conducted "at a distance" from the target and involves reflectance from either whole plants or plant canopies under natural lighting conditions. This conventional approach has yielded a wealth of information relating to characteristics of and temporal

changes occurring in the earth's land and water surfaces, but is subject to one major constraint, i.e., a requirement for suitable weather conditions (e.g., clear sunny skies) for the acquisition of most types of imagery (Gandy et al., 2011).

In certain types of studies, however, the use of leaf samples (rather than whole plants or canopies) and artificial lighting sources (rather than sunlight) may be required to obtain spectral data required to analyze certain variables or parameters. For example, Gandy (2010) evaluated the relationship between foliar reflectance by common sunflower (*Helianthus annuus* L.) and arsenic content of individual leaves. The experimental design of this particular study involved the acquisition of spectral measurements for excised individual leaves under an artificial lighting source in the laboratory followed by the immediate preservation of sample leaves for subsequent chemical analyses. Studies of this type, which involve "close-up" remote sensing under laboratory conditions require prior knowledge of several effects including: 1) the spectral properties of a suitable artificial lighting source in relation to sunlight, 2) the spectral effect(s) of various background materials and 3) the effects of leaf excision and handling methods on leaf tissues to ensure that spectral measurements obtained from excised leaf samples are biologically meaningful (for recent studies on these factors, see articles by Jensen (2007), Summy et al. (2003a, 2004, 2011), and Gandy et al. (2011)).

One factor of major importance in "close-up" remote sensing is the naturally wrinkled or curved surfaces (e.g. Gaussian curvature) of plant leaves, which may adversely impact the ability to obtain consistent data between plant species and plant samples. Gaussian surfaces are represented universally in nature. In general, simple structures, such as spheres, cylinders, and cones, exhibit constant and positive, or *synclastic*, Gaussian curvature. However, plant leaves are complex, paraboloid or free-form surfaces that exhibit synclastic and negative, or *anticlastic*, Gaussian curvature simultaneously at both "global" and "local" levels. In general, synclastic Gaussian curvature indicates that leaf growth has occurred in the center, where the edges have remained relatively fixed producing a convex, or cupped structure (Nath et al., 2003; Liu et al., 2010) (Figure 3). A leaf with synclastic Gaussian curvature exhibits increased scattering of reflected light. Light scattering (Figure 3) occurs when reflected light (θ_r) deviates significantly from its incident angle ($\theta_i \neq \theta_r$). This is type of curvature is exhibited by leaves of *Cucumis sativus* L. (cucumber) and *Glycine max* (L.) Merrill (soybean). Anticlastic Gaussian curvature is characterized by slower growth of the central portion of the leaf structure relative to the edges, e.g. the leaf may be either slightly concave, yet the edges take on a wavy or uneven appearance (Nath et al., 2003). This type of curvature may also be seen in *C. sativus* and *G. max*, but is more often observed in elongated leaf types as seed in *Lycopersicon esculentum*, *Citrus* spp., and *Ficus* spp., and monocots, including *Sorghum bicolor* (L.) Moench and *Zea mays* L. Stressors may increase synclastic and anticlastic Gaussian leaf curvature, thus increasing the need to compress the reflective Gaussian surface so as to measure treatment differences in imagery as opposed to reflectance artifacts due to curvature of the leaf. Although a typical plant canopy may contain many different leaf surfaces each existing at different angles and exhibiting different levels of Gaussian curvature, we have not attempted to address that level of complexity in this chapter. In order to assess the contributions of individual leaves to whole plant remote-sensing data, these should be reliably mounted using an *in situ* image acquisition system (Figure 4) in which (1) significant turgor loss is not observed (after leaf excision) and (2) light

scattering (defined herein as variability in angles of reflectance) is reduced after flattening. Both factors (1) and (2) could potentially influence the interpretation of remotely sensed data (Daughtry and Biehl, 1985). The purpose of the studies described in this chapter was to design and evaluate an image acquisition system where individual leaves can be remotely sensed under artificial lighting while mitigating turgor loss and leaf curvature.

2. Previous work

One of the principle advantages of CIR imagery is its ability to capture NIR wavelengths not visible by the human visual system. CIR photographs and digital CIR images consist of three broadband layers sensitive to EMR in the green, red and NIR regions of the spectrum. A ratio of NIR and red wavebands (a *simple vegetation index*) can be used to enhance acquired CIR imagery and facilitate quantitative comparison of images obtained from different treatments. This capability has been used to detect and monitor a variety of stress factors in agricultural crops, including damage caused by excess salt and moisture (Myers et al., 1963; Everitt et al., 1981; Yousef et al., 2011), nutrient deficiencies (Thomas and Oerther, 1977; Summy et al., 2003b; Yousef et al., 2011), and a variety of agricultural pests and plant diseases (Colwell, 1956; Brenchley, 1964; Norman and Fritz, 1965; Hart and Myers, 1968; Hart et al., 1973; Blazquez et al., 1979; Blazquez and Horn, 1980; Blazquez et al., 1988; Payne et al., 1971; Toler et al., 1981; Everitt et al., 1994; Everitt et al., 1996; Summy et al., 2003a Summy and Little, 2008; Summy et al., 2010).

Fungal pathogens of glasshouse plants represent a major constraint for optimum production and product quality. Significant changes in the reflected wavelengths of the near-infrared portion of the electromagnetic spectrum occur when reflectance measurements are obtained from plants infected by fungal pathogens and also from plants covered with sooty mold. Summy and Little (2008) collected data from several species of citrus seedlings (*Citrus sinensis*, *C. aurantium*, *C. paradisi* and *Poncirus trifoliata*), Bo seedlings (*Ficus religiosa*), and cantaloupe (*Cucumis melo reticulata*) propagated under natural lighting conditions in the glasshouse. Spectroradiometric measurements and color infrared (CIR) images of control, honeydew only, and sooty molded leaves from *F. religiosa*, *C. sinensis*, *C. aurantium*, and *P. trifoliata* were obtained. *C. paradisi* infected with the greasy spot fungus (*Mycosphaerella citri*) was also imaged under glasshouse lighting. Similar data was obtained from healthy foliage of *C. melo reticulata* and foliage with various levels of powdery mildew (*Sphaerotheca fuliginea*) infection.

Summy and Little (2008) assessed the relative levels of visible and near-infrared (NIR) reflectance from plants infested with sooty mold (coated with insect honeydew) and infected with fungal pathogens versus respective controls, under glasshouse conditions. Both "control" and "treated" whole plants and single leaves were imaged using conventional color and color infrared (CIR) photography

Although differences were observed when looking at leaves that were coated in honeydew only, accumulations of honeydew on leaf surfaces generally presented the same trends between plant species and different depositors. For example, NIR/red ratio images showed a significant decrease in reflectance when comparing sooty-molded plants versus "clean" controls. This relationship was sustained in three of the citrus species tested (*P. trifoliata*, *C. aurantium*, and *C. sinensis*) as well as "bo" tree seedlings (*F. religiosa*). This trend is

accentuated when observing the individual contributions of particular leaves with varying levels of sooty mold after being mounted on the *in situ* image acquisition system. The reason for the decrease in NIR reflectance is due to the growth of dematiaceous (dark) fungal hyphae on the honeydew substrate. The resulting "mat" of fungal hyphae absorbed NIR light as opposed to reflecting it. Dematiaceous hyphae, which characterize the Capnodiaceae (including *Capnodium* spp.), contain significant amounts of melanin giving the sooty mold its dark color. Melanin is a polymer of indoles and tyrosine conversion intermediates that function in fungi and animals to absorb light and protect against irradiative damage (Riley, 1998). Therefore, it is not surprising that reflectance should decrease significantly from sooty-mold infested plant leaves. In fact, the absorption maxima of melanins derived from several dematiaceous ascomycetes and deuteromycetes have been shown to absorb red (400 to 500 nm), infrared (> 700 nm), and UV-B (280 to 315 nm) wavelengths (Bell and Wheeler, 1986; Babitskaya and Shcherba, 2002).

Summy and Little (2008) also tested leaves of varying ages from trifoliate orange (*P. trifoliata*) and sour orange (*C. aurantium*). In the case of trifoliate orange, there was no difference between NIR/red ratio images of 20 d or 35 d old leaves. However, sour orange differed in that the greatest NIR/red ratios were seen in 20 d old leaves and differed significantly from the 10 d and 35 d leaves.

A number of studies have demonstrated the ability to detect the red and NIR reflectance changes of plant tissues associated with fungal pathogens in the field (Colwell, 1956; Brenchley, 1964; Norman and Fritz, 1965). However, there is very little information concerning pathogen detection using CIR imagery and analysis in the glasshouse setting. Summy and Little (2008) considered two examples of foliar diseases: (1) powdery mildew of cucurbits (*Sphaerotheca fuliginea*) and (2) greasy spot of citrus (*Mycosphaerella citri*).

The powdery mildew diseases are characterized by extensive white fungal growth on the upper surface of the plant leaf. The "powdery" appearance is due to the production of numerous conidia and conidiophores. It is hypothesized that incident radiation that comes in contact with the fungal structures is both scattered *and* absorbed. Scattering may be due to the random placement of conidiophores on the leaf surface leading to an infinite number of angles at which light may be reflected. Absorption may occur due to small water droplets that are trapped between the fungal hyphae and the conidiophores. Summy and Little (2008) showed a significantly reduced NIR/red ratio and lower NIR reflectance in leaves infected with powdery mildew. This is an area requiring further study.

Decreases in NIR/red ratios in the case of leaf chlorosis appear to be quite common whether the stress is abiotic or biotic in nature. Chlorosis (see above) is a primary symptom that accompanies pseudothecium (fungal sexual fruiting structure) development in the greasy spot disease of citrus. Summy and Little (2008) indicated that red reflectance increases as greasy spot severity increased, whereas NIR reflectance did not appear to change appreciably, thus the NIR/red ratios decreased.

Color infrared (CIR) and multispectral imagery have been used for many years to assess damage caused by insect and mite infestations in conventional (outdoor) agricultural crops, but have not been used for this purpose to any extent within the commercial glasshouse environment or to evaluate individual leaves. In an effort to evaluate the potential of CIR imagery for detection and monitoring of arthropod infestations on glasshouse plants,

Summy et al. (2010) assessed spectral changes in foliage occurring in response to damage caused by three common glasshouse pests: 1) citrus mealybug, *Planococcus citri* (Pseudococcidae), 2) California red scale, *Aonidiella aurantii* (Diaspididae) and 3) carmine mite, *Tetranychus cinnabarinus* (Tetranychidae). Damage caused by each of these representative pest species resulted in distinct spectral signatures that were distinguishable from those of healthy foliage in both spectroradiometer measurements and CIR imagery (see examples in Figure 1). Potential applications of CIR imagery for the detection and monitoring of insect and mite infestations on glasshouse are discussed below.

Ornamental plants and vegetable crops produced commercially under glasshouse conditions are subject to infestation by most, if not all, of the insect and mite pests that are associated with these same crops in conventional (outdoor) plantings. Pest infestations developing on glasshouse crops commonly occur under near-optimal environmental conditions, which may include an absence of natural enemies (predators, parasites and pathogens) that provide a measurable degree of control in field infestations. As a result, insect and mite infestations developing within the protected glasshouse environment commonly exhibit relatively high rates of increase that provide a potential to cause levels of damage equivalent to or greater than those occurring in conventional field situations. Thus, effective management of such pests is predicated, in part, on the availability of efficient survey methodology designed to provide the glasshouse manager with timely and accurate information regarding the occurrence and current status of pest infestations, and the need (or lack thereof) for suppression measures. In order to be feasible, any such survey methodology must provide accurate information in near real-time and must be usable under all weather and lighting conditions. In addition, such methodology should be relatively inexpensive and simple to use.

Citrus mealybug, *Planococcus citri* (Hemiptera: Pseudococcidae), is one of the most serious insect pests associated with citrus and numerous ornamentals grown under glasshouse conditions. Damage results from the combined effects feeding activities (i.e., extraction of sap via sucking mouthparts) and excretion of copious quantities of honeydew (a sugary waste product), which accumulate on leaves and serve as a medium for sooty mold fungus. Dense deposits of sooty mold fungi may attenuate a significant portion of the electromagnetic radiation (EMR) incident on leaves. This is an effect that tends to severely retard photosynthesis. Field populations of *P. citri* on citrus in southern Texas and other areas are normally regulated at subeconomic densities by a complex of predators and parasites (Ancisco et al., 2002), although these are typically lacking in glasshouse infestations.

Summy and Little (2008) provided a comprehensive discussion of the spectral changes in foliage associated with the accumulation of honeydew and development of sooty mold deposits on foliage of citrus and other plants. One particularly important trend reported in that study relates to the observation that honeydew accumulations on foliage tend to increase NIR reflectance (with little or no apparent effects in reflectance in the visible region), whereas sooty mold deposits tend to decrease NIR reflectance and increase reflectance of wavelengths in the blue and red regions of the spectrum. Leaves contaminated with honeydew and sooty mold deposits were distinguishable from undamaged leaves in CIR imagery, and their presence on foliage was particularly evident in ratio (NIR/R) images. The capability of CIR and derivative imagery to detect honeydew deposits on foliage should be particularly useful in detection of incipient (low-density) infestations of *P.*

citri and other "honeydew excretors," including the soft scales (Coccidae), aphids (Aphididae), and whiteflies (Aleyrodidae).

Summy et al. (2010) found that although uninfested mature and immature *Citrus sinensis* leaves were distinguishable in the conventional color (RGB) image, no differences in coloration were evident among a series of mature leaves exhibiting a range of scale insect (A. *aurantii*) densities. These observations were consistent with spectroradiometer measurements, which detected no significant differences in reflectance of visible wavelengths among the series of infested mature leaves. In the CIR composite image, the presence of scale armor on infested foliage was indicated by a distinct speckling pattern. Although spectral curves for infested leaves indicated a significant reduction in NIR reflectance with increases in scale densities, only subtle differences in coloration of infested foliage were evident in the CIR composite image. However, evidence of physiological stress in infested leaves was evident in a ratio image which indicated high ratios of NIR:R in uninfested leaves and low ratios in infested leaves. Similar trends were evident in imagery of a Valencia orange tree acquired at a distance of 2.5 m under natural lighting conditions. The presence of scale armor on leaves was detectable in the conventional color image and was very conspicuous in the CIR composite image. Although differences in leaf coloration were very subtle in both RGB and CIR images, a ratio image indicated high NIR:R ratios for uninfested or lightly-infested leaves, and lower ratios for heavily infested leaves, many of which exhibited ratios similar to those of background reflection.

Spider mites (Acari: Tetranychidae) rank among the most chronic and potentially destructive pests of vegetable crops and ornamentals grown in commercial glasshouses. Damage results from the destruction of leaf epidermal tissue, which produces a distinctive "mottled" appearance of infested foliage. As a result of their short developmental times and high fecundities, spider mite infestations tend to increase rapidly to damaging levels, which may result in substantial damage and/or defoliation of glasshouse plants. A number of predaceous mites, e.g., *Phytoseiulus persimilis* (Acari: Phytoseiidae), have been shown to be effective in spider mite control and are produced commercially for this purpose (Yepsen, 1984), although these typically require introduction into the glasshouse environment.

Summy et al. (2010) found that differences in coloration between undamaged *Cucumis sativus* leaves and those exhibiting a slight degree of carmine spider mite (*T. cinnabarinus*) damage were very subtle and difficult to distinguish in RGB imagery, while leaves exhibiting moderate and intense damage were distinguishable. Similar trends were evident in the CIR composite image. These observations were consistent with spectroradiometer measurements, which indicated significantly higher levels of reflectance of visible wavelengths from the damaged leaf relative to the undamaged control, and a substantial and progressive increase in reflectance of visible wavelengths as the extent of tissue damage increased. Although an analysis of variance detected one significant difference in reflectance at 850 nm, the similarity of NIR reflectance among the remaining groups (i.e., undamaged controls and those exhibiting slight and intense damage) suggests that mite feeding injury did not influence this parameter.

Summy et al. (2010) showed that the rapidity at which mite damage increased between two late sampling dates exemplifies the destructive potential of spider mites in the glasshouse environment and the need to detect such infestations while they are still at the incipient

stage, i.e., have not increased to damaging levels. Such infestations exhibit an aggregated distribution and may occur at densities too low to produce symptoms that are readily detectable through visual inspection or use of conventional photographic techniques. Leaves exhibiting a low intensity of spider mite damage were difficult to distinguish from undamaged foliage using either conventional RGB or CIR imagery alone; the two were highly distinguishable in a simple ratio image.

Summy et al. (2010) found that increases in the intensity of mite damage to leaves were accompanied by progressively higher levels of visible (blue, green and red) reflectance with little or no change in NIR reflectance. The effects of these spectral changes were clearly evident in the ratio image in which increasing intensity of mite damage was accompanied by progressively decreasing ratios of NIR to red wavelengths. The significance of this trend relates to the fact that the undamaged control and the slightly damaged leaf, which were not readily distinguishable in either the RGB or CIR images, were clearly distinguishable in the ratio image.

Numerous studies have indicated the occurrence of spectral changes in stressed plants including those due to nitrogen deficiency and soil salinity in conventional crops. Blackmer et al. (1996) detected nitrogen deficiency in corn (*Z. mays*) in the green region of the spectrum at a wavelength of 550 nm. Osborne et al. (2002) predicted the nitrogen concentration form corn canopies by using reflectance in the green and red regions of the spectrum. Gausman et al. (1985) stated that soil salinity stress in cotton (*Gossypium* spp.) plants cause spectral changes and can be detected using CIR imagery. Leone et al. (2000) was able to detect soil salinity in pepper plants (*Capsicum annuum* L.) using spectral reflectance measurements. Nonetheless, very limited research has been conducted to evaluate the potential of using remote sensing techniques in detecting nitrogen deficiency and soil salinity stresses in greenhouse crops.

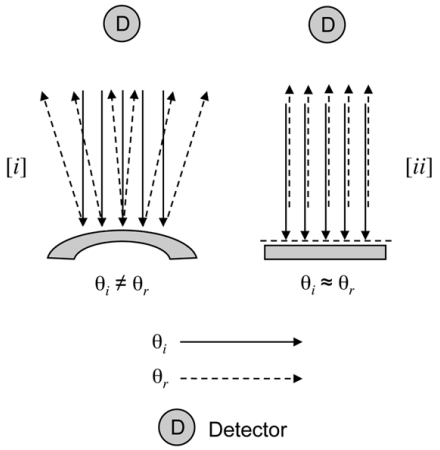

Fig. 3. Reduction of light scattering [*i*] results when leaves exhibiting synclastic Gaussian curvature are compressed [*ii*]. Compression of the leaves using the *in situ* image acquisition template results in light reflected at angles (θ_r) equivalent or nearly so to incident light (θ_i), which improves the quality of sample detection via image acquisition or spectroradiometry.

3. Methodology

In order to assess the contributions of individual leaves to whole plant remote-sensing data, leaf samples were mounted using an *in situ* image acquisition system in which significant turgor loss is not observed (after leaf excision) and light scattering (defined as the variability in angles of reflectance) is reduced after compression of a reflective Gaussian surface (Figures 3 and 4). Light scattering occurs when reflected light deviates significantly from its incident angle ($\theta_i \neq \theta_r$; where θ_i = angle of incidence, θ_r = angle of reflectance) (Figure 3).

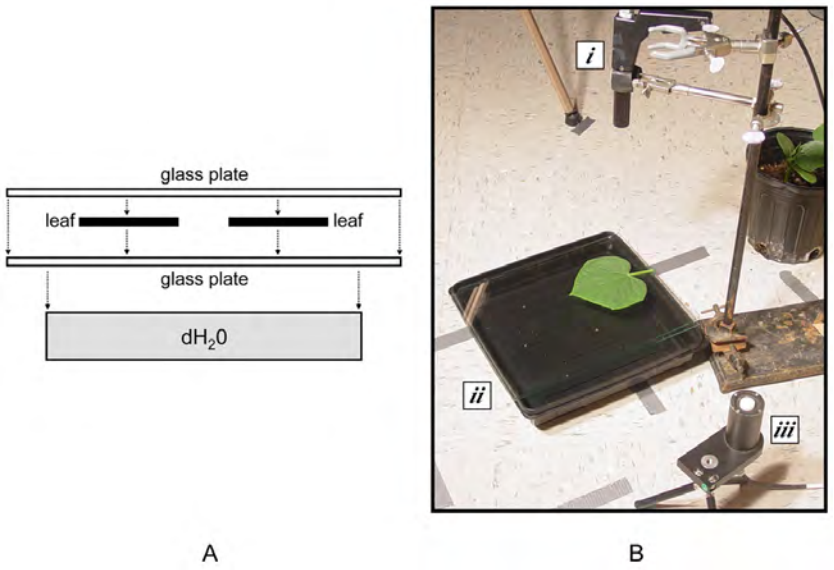

Fig. 4. Diagram of the *in situ* image acquisition template used to examine individual leaves acquired from healthy and stressed whole plants (A). Photo of the image acquisition template demonstrating the use of the [*i*] VNIR sensor, [*ii*] glass plates, and [*iii*] remote cosine receptor used to collect spectrophotometric data (B). A CIR camera may be mounted at the same level as the spectroradiometer VNIR sensor shown above [*i*].

For the studies described in Summy and Little (2008) and Summy et al. (2010), vertical CIR images of individual leaves mounted using a plexiglass template were acquired under natural and artificial lighting conditions (500 W halogen lamps) at a distance of 1.5 m using a DuncanTech MS3110 digital CIR camera. CIR imagery acquired in this manner was imported into an image-processing package (Idrisi32® or Kilamanjaro®) after being converted to ".TIF" files and separated into NIR, red, and green bands using Adobe Photoshop 7. CIR imagery was evaluated to determine the degree to which the color rendition of infected and infested plants of a given species or cultivar differs from healthy controls in the raw (unprocessed) CIR imagery. Conventional CIR photography was also used for some experiments. In this case, a 35 mm Nikon SLR camera equipped with a Wratten 15 (yellow) filter and loaded with Kodak Ektachrome Professional Infrared EIR film

were used to obtain the CIR images described in this chapter. All RGB "control" images were captured using a Sony Mavica CD400 digital camera.

In order to obtain NIR/red ratios, simple vegetative indices were generated utilizing the red and NIR bands of images that had been converted from digitized CIR images in Idrisi32®. The resulting images represent a ratio of NIR and red *at each pixel*. Ratio images were contrast stretched where necessary in order to eliminate approximately 20% of the unrepresentative wavelengths. To statistically compare NIR/red ratio images, contrast stretched ratios images were layered with a stratified spatial sample of random points. For individual leaves, 20 random points were selected. NIR/red ratio random point means, from template-mounted leaves, were compared using ANOVA and a means separation test (Tukey's Honestly Significant Difference ($P < 0.05$)).

Spectral measurements of healthy plants and plants within treatment or exposure groups (abiotic and biotic stressors) were obtained under natural and artificial lighting conditions using a FieldSpec VNIR spectroradiometer equipped with a remote cosine receptor (Analytical Spectral Devices, Boulder, CO) to measure incident radiation between the ultraviolet (350 nm) and NIR (1100 nm) regions of the electromagnetic spectrum. The spectroradiometer was equipped with ViewSpec Pro software (Analytical Spectral Devices, Boulder, Colorado). Measurements of radiance were converted to percent reflectance using a Spectralon® reference plate, and reflectance of selected wavelengths in the blue (450 nm), green (550 nm), red (650 nm) and NIR regions (850 nm) were compared using ANOVA and a means separation test (Tukey's HSD, $P < 0.05$).

The *in situ* image acquisition system used in these studies (Figure 4) consisted of a black, plastic plant growth flat filled with distilled water (in order to absorb light and prevent background reflection in images) and two 0.3 x 22 x 30 cm glass plates. Individual leaves were pressed between the glass plates and then remotely sensed using spectroradiometry and CIR imagery (Figure 4). The glass plates used in the "template system" were evaluated for irradiance levels (350 to 1150 nm) to check the relative amount of light attenuation that might occur in various wavebands due to the layer of glass covering a leaf held on the template (Figure 4).

To test the effect of leaf excision, *L. esculentum* and *C. sativus* non-excised and excised leaves were measured with the Field Spec Dual VNIR spectroradiometer when pressed between the glass plates on the *in situ* image acquisition system. Measurements were taken at 0, 1, 2, 3, 4, and 5 minutes after excision. Mean NIR/red ratio values were derived from ratio images (simple vegetation indices, see below) of excised and non-excised *L. esculentum* and *C. sativus* leaves that either were or were not flattened using the image acquisition system (Tables 1 and 2). Individual leaves were flattened between two glass plates using the *in situ* image acquisition system previously described. Spectoradiometer data and CIR imagery were obtained and analyzed. Measurements were taken 10 and 12 minutes after excision.

The quality and interpretability of CIR imagery acquired under an artificial (quartz halogen) lighting source is comparable to that acquired under natural lighting conditions, which clearly demonstrates that ambient lighting conditions do not pose a major constraint to the use of this technology for monitoring pest infestations in the glasshouse environment (Summy et al., 2004).

4. Results and progress

Leaves may be excised and data obtained without loss of spectral and image data quality if data is obtained in a relatively brief period of time. Leaf excision did not significantly reduce spectroradiometric values from either *C. sativus* or *L. esculentum* compared to non-excised leaves. Also, NIR/red ratio means did not differ when comparing non-excised and excised. There was a significant difference between spectroradiometric and NIR/red ratio values between compressed and non-compressed leaves using the *in situ* image acquisition system, whether comparing differences in Gaussian leaf curvature or plant stressors. Specifically, leaf compression generally reduced variability (standard deviations) among the quantitative spectroradiometric and imagery data, which improved the ability to differentiate treatment effects (Tables 1 and 2).

Treatment	**NIR/red ratio (Mean ± SD)**
Non-excised, non-flattened	2.69 ± 0.33 a*
Non-excised, flattened	2.49 ± 0.21 b
Excised, flattened	2.40 ± 0.15 b

Table 1. Mean NIR/red ratio values derived from ratio images of excised and non-excised *C. sativus* leaves flattened or not flattened using the *in situ* image acquisition system. *Values followed by different letters are significantly different at $P < 0.05$ (Tukey's HSD).

Treatment	**NIR/red ratio (Mean ± SD)**
Low curvature, non-flattened	2.57 ± 0.67 a*
High curvature, non-flattened	2.18 ± 0.55 bc
Low curvature, flattened	2.31 ± 0.26 ab
High curvature, flattened	1.93 ± 0.21 c

Table 2. Mean NIR/red ratio values derived from ratio images of excised *L. esculentum* leaves exhibiting low or high Gaussian curvature flattened or non-flattened using the *in situ* image acquisition system. *Values followed by different letters are significantly different at $P < 0.05$ (Tukey's HSD).

Treatment	**NIR/red ratio (Mean ± SD)**
Healthy, non-flattened	2.59 ± 0.14 a*
-N, non-flattened	1.46 ± 0.19 c
Healthy, flattened	2.19 ± 0.15 b
-N, flattened	1.37 ± 0.16 c

Table 3. Mean NIR/red ratio values derived from ratio images of healthy or N deficient (-N) excised *C. sativus* leaves flattened or non-flattened using the *in situ* image acquisition system. *Values followed by different letters are significantly different at $P < 0.05$ (Tukey's HSD).

Use of the *in situ* image acquisition system successfully aided the acquisition of color infrared imagery and spectroradiometric data from *Citrus* spp., *Ficus religiosa*, *C. sativus*, and *L. esculentum* exposed to biotic stressors, including fungi and insects. The *in situ* image acquisition system described in this chapter and utilized in Summy and Little (2008) and Summy et al. (2010) showed two important features that suggest a potential application to understanding the contributions that individual leaves make to a holistic remote sensing image. Leaves may be excised and data obtained without loss of spectral quality if data is obtained in a relatively brief period of time. Water potential in leaves is regulated by two mechanisms: (1) opening and closing of the stomata and (2) internal osmotic pressure differentials in the vasculature of the plant (and associated cells) (Gutschick, 1999). Leaf excision did not significantly reduce spectroradiometric values from either *L. esculentum* or *C. sativus* compared to non-excised leaves (Figure 5). Also, NIR/red ratio means did not differ when comparing non-excised and excised (Table 1).

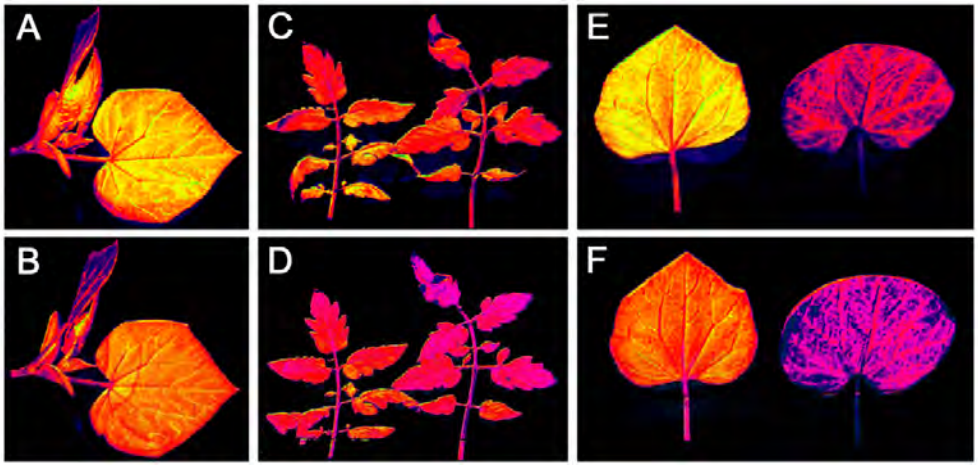

Fig. 5. False-colored near-infrared/red ratio images of non-excised *Cucumis sativus* leaves (A) non-flattened and (B) flattened using the *in situ* image acquisition system (see Fig. 4). Near-infrared/red ratio images of excised (left-side of panels) and non-excised (right-side of panels) *Lycopersicon esculentum* leaves before (C) and after (D) flattening, respectively. Near-infrared/red ratio images of healthy *C. sativus* leaves (left-side of panels) and those exhibiting nitrogen deficiency (right-side of panels) before (E) and after flattening (F).

There was a significant difference between spectroradiometric and NIR/red ratio values between leaves that were and were not flattened using the "template system" whether comparing differences in leaf curvature or plant stress (Figures 5 and 6; Tables 1, 2, and 3). However, it is difficult to visualize the differences when comparing NIR/red ratio images though changes in the uniformity of the images are observed. This increase in uniformity of the flattened leaves is demonstrated by the decrease in variability (eg. standard deviations) among quantitative data derived from the NIR/red ratio images (Tables 1, 2, and 3).

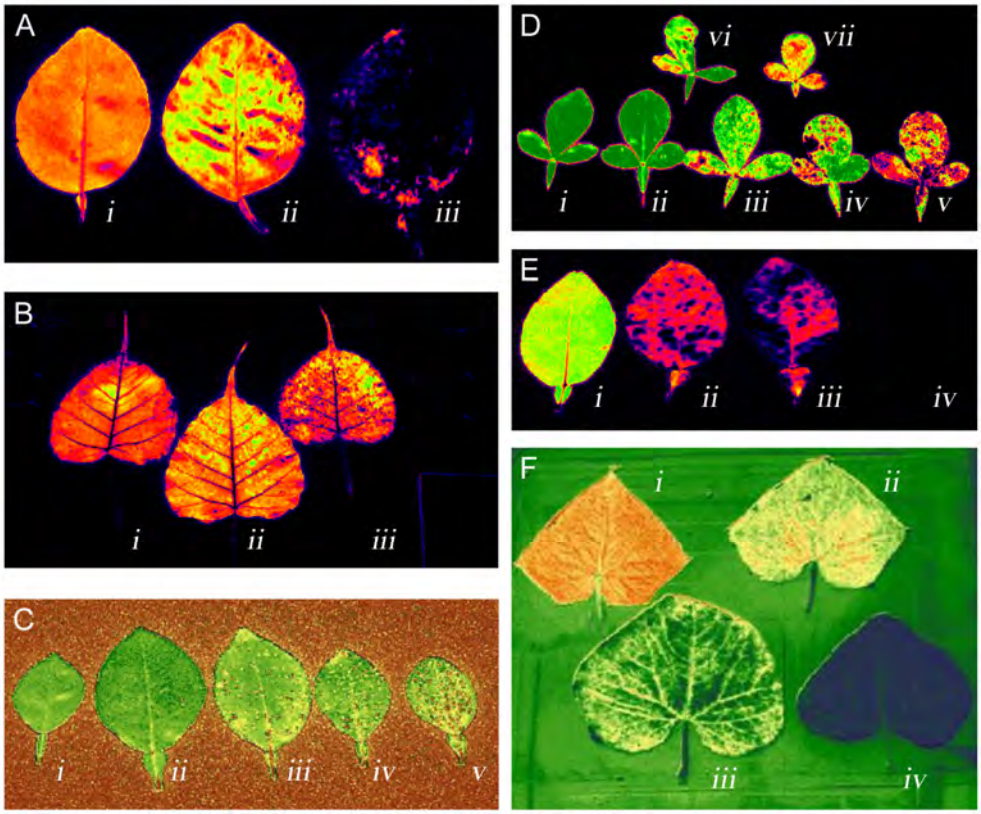

Fig. 6. Examples of false-colored NIR/red waveband ratio images of excised leaves from healthy and stressed plants acquired using the *in situ* image acquisition template. (A) Healthy [*i*], insect honeydew-coated [*ii*], and sooty mold infested [*iii*] 'Valencia' orange [*Citrus sinensis*] leaves; (B) Healthy [*i*], honey-dew coated [*ii*], and sooty mold infested [*iii*] *Ficus religiosa* leaves; (C) 'Valencia' orange leaves non-infested [*i, ii*] and infested [*iii, iv, v*] with California red scale insect armor [*Aonidiella aurantii*]; (D) Healthy [*i, ii*], and sooty mold and citrus mealy bug [*Planococcus citri*] infested [*iii-vii*] trifoliate orange [*Poncirus trifoliata*] leaves. The leaflets in item *v* represent the highest level of infestation; (E) Healthy [*i*] and diseased [*ii-iv*; greasy spot, *Mycosphaerella citri*] grapefruit leaves. Severe chlorosis in item *iv* resulted in a NIR/red ratio coded as black in the false-colored image; (F) Healthy [*i*] and spider mite [*Eutetranychus banksi*] damaged [*ii-iv*] cucumber leaves [*C. sativus*] leaves.

5. Opportunities and constraints

The common use of NIR/red ratio images to detect plant stress is based on the well known fact that stressed plants commonly exhibit both a decrease in NIR reflectance and an increase in reflectance of red wavelengths. Thus, NIR/red ratios tend to be relatively high within areas of imagery representing healthy plant foliage, and generally decrease within areas exhibiting physiological stress. The main exception to this is significant honeydew deposition on leaf surfaces. Ratio images compiled during the research described clearly demonstrate the potential usefulness of this image enhancement technique for identifying certain types of biotic plant stress.

Damage caused by each of the representative pest species discussed herein was accompanied by distinct spectral changes that were readily distinguishable (from healthy foliage) in CIR and/or derivative imagery. By providing a capability to identify small and localized areas of foliar damage (e.g., feeding injury by spider mites) and/or the presence of characteristic pest products on plants (e.g., honeydew), CIR imagery appears to have considerable potential for the detection of incipient infestations of several major groups of glasshouse arthropod pests. Moreover, use of a suitable artificial lighting source (e.g., quartz halogen lamps) facilitates the acquisition of CIR imagery that is equivalent in quality and interpretability to imagery obtained under optimal natural lighting conditions, and thus mitigates a major problem (i.e., poor or unpredictable ambient lighting) that has long represented one of the principal constraints to use of remote sensing in conventional outdoor crops.

Overall it appears that excising and flattening leaves do not severely affect spectroradiometric and CIR image quality. Thus, one of the principal advantages of this method is that it provides a means by which to experimentally compare reflectance values and image ratios (NIR/red) in "side-by-side" comparisons without the vagaries caused by leaf curvature or reflectance from adjacent or underlying leaves. Summy and Little (2008), Summy et al. (2010), and Yousef et al. (2011) discuss the use of this template system for the direct comparison of leaves exhibiting signs and symptoms of sooty mold and fungal pathogens, insect infestations, and nutrient deficiencies and toxicities.

6. Future directions

In order to effectively use a template system such as that described herein for obtaining accurate spectral measurements of excised leaves, the user must ensure that the excision process and handling methods for leaf samples do not adversely affect leaf tissues or cause a degree of desiccation sufficient to affect spectral reflectance (Foley et al., 2006). Although much emphasis has been placed on laboratory handling methods, the procedures used to store samples for transport to the laboratory are equally important. One recent study demonstrated that excised foliage of giant reed, *Arundo donax*, placed within paper bags and stored in a refrigerated ice chest desiccated rapidly and exhibited substantial changes in spectral properties within a period of 24 hours following collection. In contrast, samples of *A. donax* foliage stored within clear plastic zip-lock bags exhibited little evidence of desiccation or significant changes in spectral properties for 72 to 96 hours after collection (Summy et al., *in press*) (Figure 7). The development of field collection and transport

methodology for plant foliage is critical to obtaining accurate spectral measurements in the laboratory and represents a fruitful area of future research.

Fig. 7. Samples of *Arundo donax* leaves maintained in plastic zip-lock bags (*left*) and paper bags (*right*) following a 96-hour observation period (from Summy et al., *in press*).

7. Acknowledgements

This book chapter is Contribution No. KAES 12-084-B from the Kansas Agricultural Experiment Station, Manhattan.

8. References

Ancisco, J.R., French, F.V., Skaria, J.W., and Holloway, R. (2002). IPM in Texas citrus. Texas Cooperative Extension Service, B-6121. Texas A&M University, College Station, Texas, USA

Avery, T.E., and Berlin, G.L. (1992). *Fundamentals of remote sensing and airphoto interpretation*, 5th ed. Prentice Hall, ISBN 0-02305-035-7, Upper Saddle River, New Jersey, USA

Babitskaya, V.G., and Shcherba, V.V. (2002). The nature of melanin pigments of several micro- and macromycetes. *Applied Biochemistry and Microbiology*, Vol. 38, No. 3, pp. 411-451

Bell, A.A., and Wheeler, M.H. (1986). Biosynthesis and function of fungal melanins. *Annual Review of Phytopathology*, Vol. 24, No. 1, pp. 411-451

Blackmer, T.M., Schepers, J.S., Varvel, G.E., and Walter-Shea, E.A. (1996). Nitrogen deficiency detection using reflected shortwave radiation for irrigated corn canopies. *Agronomy Journal*, Vol. 88, No. 1, pp. 1-5

Blazquez, C.H., and Horn, F.W. (1980). Aerial color infrared photography: applications in agriculture. National Aeronautics and Space Administration, Reference Publication 1067, Washington, D.C.

Blazquez, C.H., Edwards, G.J., and Horn, F.W. (1979). Aerial color infrared photography - a management tool. *Florida State Horticultural Society Proceedings*, Vol. 92, No. 1, pp. 13-15

Blazquez, C.H., Lowe, O., Sisk, J.R., and Bilbrey, M.D. (1988). Use of aerial color infrared photography, dual color video, and a computer system for property appraisal of

citrus groves. Photogrammetry Engineering and Remote Sensing, Vol. 54, No. 2, pp. 233-236

Brenchley, G.H. (1964). Aerial photography for the study of potato blight. *World Review of Pest Control*, Vol. 3, No. 1, pp. 68-84

Campbell, J.B. (2002). *Introduction to remote sensing*, 3rd ed. Guilford Press, ISBN 1-57230-640-8, New York, New York, USA

Colwell, R.N. (1956). Determining the prevalence of certain cereal diseases by means of aerial photography. *Hilgardia*, Vol. 26, pp. 223-226

Cracknell, A.P., and Hayes, L. (2007). Introduction to remote sensing, 2nd ed. CRC Press, ISBN 0-84939-255-1, Boca Raton, Florida, USA

Daughtry, C.S.T., and Biehl, L.L. (1985). Changes in spectral properties of detached birch leaves. *Remote Sensing of the Environment*, Vol. 17, No. 3, pp. 281-289

Everitt, J.H., Drawe, D.L., Little, C.R., and Lonard, R.I. (2011). *Grasses of south Texas: a guide to their identification and value.* Texas Tech University Press, ISBN 0-89672-668-1, Lubbock, Texas, USA

Everitt, J.H., Gerbermann, A.H., and Alaniz, M.A. (1981). Microdensitometry to identify saline rangelands on 70 mm color infrared film. *Photogrammetric Engineering and Remote Sensing*, Vol. 47, pp. 1357-1362

Everitt, J.H., Lonard, R.I., and Little, C.R. (2007). *Weeds in south Texas and northern Mexico: a guide to identification.* Texas Tech University Press, ISBN 0-89672-614-2, Lubbock, Texas, USA

Foley, S., Rivard, B., Sanchez-Azofeifa, and Calvo, J. (2006). Foliar spectral properties following leaf clipping and implications and implications for handling techniques. *Remote Sensing of the Environment*, Vol. 103, pp. 421-425

Forterre, Y., Skotheim, J.M., Dumais, J., and Mahadevan, L. (2005). How the Venus flytrap snaps. *Nature*, Vol. 433, pp. 421-425

Gamon, J.A., and Surfus, J.S. (1999). Assessing leaf pigment content with a reflectometer. *New Phytologist*, Vol. 143, No. 1, pp. 105-117

Gandy, Y.P.P. (2010). Spectral reflectance as an indicator of foliar concentrations of arsenic in common sunflower, *Helianthus annuus*. *M.S. Thesis*, The University of Texas - Pan American, Edinburg, Texas, USA

Gandy, Y.P., Mamachen, A., Mamachen, A., Lieman, J., Persans, M., Parson, J., Ibrahim, E., Summy, K.R., and Little, C.R. (2011). Techniques to facilitate the acquisition of accurate spectral measurements and multispectral imagery of plant foliage under artificial lighting conditions. *Subtropical Plant Science*, Vol. 63, No. 1 (*in press*)

Gates, D.M., Keegan, J.J., Schleter, J.C., and Weidner, V.R. (1965). Spectral properties of plants. *Applied Optics*, Vol. 4, No. 1, pp. 11-20

Gausman, H.W., Allen, W.A., and Cardenas, R. (1969). Reflectance of cotton leaves and their structure. *Remote Sensing of the Environment*, Vol. 1., No. 1, pp. 110-122

Gausman, H.W. (1985). Plant leaf optical parameters in visible and near-infrared light. *Graduate Studies, Texas Tech University, No. 29*. Texas Tech University Press, ISBN 0-89672-132-9, Lubbock, Texas, USA

Gutschick, V.P. (1999). Biotic and abiotic consequences of differences in leaf structure. *New Phytologist*, Vol. 143, No. 1, pp. 3-18

Hart, W.G., and Myers, V.I. (1968). Infrared aerial color photography for the detection of populations of brown soft scale in citrus groves. *Journal of Economic Entomology*, Vol. 61, No. 3, pp. 617-624

Hart, W.G., Ingle, S.J., Davis, M.R., and Magnum, C. (1973). Aerial photography with infrared color film as a method of surveying for citrus blackfly. *Journal of Economic Entomology*, Vol. 66, No. 1, pp. 190-194

Jensen, J.R. (2004). *Introductory digital image processing: a remote sensing perspective,* 3rd ed. Prentice Hall, ISBN 0-13145-361-0, Upper Saddle River, New Jersey, USA

Jensen, J.R. (2006). *Remote sensing of the environment: an Earth resource perspective,* 2nd ed. Prentice Hall, ISBN 0-13188-950-8, Upper Saddle River, New Jersey, USA

Johannsen, C.J., Carter, P.G., Morris, D.K., Erickson, B., and Ross, K. (1999). Potential applications of remote sensing. *Site-specific Management Guidelines Series, SSMG-22.* Potash and Phosphate Institute, South Dakota State University, Brookings, South Dakota, USA

Lee, K., Avondo, J., Morrison, H., Blot, L., Stark, M., Sharpe, J., Bangham, A., and Coen, E. (2006). Visualizing plant development and gene expression in three dimensions using optical projection tomography. *The Plant Cell*, Vol. 18, No. 9, pp. 2145-2156

Leone, A.P., Menenti, M., and Sorrentino, G. (2001). Reflectance spectrometry to study crop response to soil salinity. *Italian Journal of Agronomy*, Vol. 4, No. 2, pp. 75-85

Lillesand, T.M., Kiefer, R.W., and Chipman, J. (2007). *Remote sensing and image interpretation,* 6th ed. John Wiley and Sons, Inc., ISBN 0-47005-245-7, New York, New York, USA

Liu, Z., Jia, L., Mao, Y., and He, Y. (2010). Classification and quantification of leaf curvature. *Journal of Experimental Botany*, Vol. 61, No. 10, pp. 2757-2767

Myers, V.I. (1970). Soil, water and plant relations. pp. 253-297 In *Remote sensing with special reference to agriculture.* National Academy of Sciences, Washington, D.C., USA

Myers, V.I., Ussery, L.R., and Rippert, W.J. (1963). Photogrammetry for detailed detection of drainage and salinity problems. *American Society of Agricultural Engineers*, Vol. 6, No. 4, pp. 332-334.

Murtha, P.A. (1978). Remote sensing and vegetation damage: a theory for detection and assessment. *Photogrammetry, Engineering & Remote Sensing*, Vol. 44, No. 9, pp. 1147-1158

Nath, U., Crawford, B.C.W., Carpenter, R. and Coen, E. (2003). Genetic control of surface curvature. *Science*, Vol. 299, No. 5611, pp. 1404-1407

Niklas, K.J. (1999). A mechanical perspective on foliage leaf form and function. *New Phytologist*, Vol. 143, No. 1, pp. 19-31

Norman, G.G., and Fritz, N.L. (1965). Infrared photography as indicator of disease and decline in citrus. *Florida State Horticultural Society Proceedings*, Vol. 75, No. 1, pp. 59-63

Osborne, S.L., Schepers, J.S., Francis, D.D., and Schlemmer, M.R. (2002). Detection of phosphorus and nitrogen deficiencies in corn using spectral radiance measurements. *Agronomy Journal*, Vol. 94, No. 6, pp. 1215-1221

Payne, J.A., Hart, W.G., Davis, M.R., Jones, L.S., Weaver, D.J., and Horton, B.D. (1971). Detection of peach and pecan pests and diseases with color infrared photography. *Proceedings of the 3rd Bienniel Workshop on Color Aerial Photography*

in the Plant Sciences, Falls Church, Virginia, USA, American Society of Photogrammetry

Perez, J.L., French, J.V., Summy, K.R., Baines, A.D., and Little, C.R. (2009). Fungal phyllosphere communities are altered by indirect interactions among trophic levels. *Microbial Ecology*, Vol. 57, No. 4, pp. 766-774

Riley, P.A. (1998). Melanin. *International Journal of Biochemistry and Cell Biology*, Vol. 29, No. 11, pp. 1235-1239

Prusinkiewicz, P., de Reuille, P.B. (2010). Constraints of space in plant development. *Journal of Experimental Botany*, Vol. 61, No. 8, pp. 2117-2129

Summy, K.R., Lieman, J., Gandy, Y.P., Mamachen, A., Mamachen, A., Goolsby, J., and Moran, P.J. (2011). Effects of leaf excision and sample storage methods on spectral reflectance by foliage of giant reed, *Arundo donax*. Subtropical Plant Science, Vol. 63, No. 1 (*in press*)

Summy, K.R., and Little, C.R. (2008). Using color infrared imagery to detect sooty mold and fungal pathogens of glasshouse-propagated plants. *HortScience*, Vol. 43, No. 5, pp. 1485-1491

Summy, K.R., Little, C.R., French, J.V., Setamou, M., Mata, J., and Everitt, J.H. (2007). Use of ratio images to detect subtle forms of plant stress caused by foliar feeding arthropods. *Proceedings of the 21st Biennial Workshop on Aerial Photography, Videography, and High Resolution Digital Imagery for Resource Assessment*. ISBN 1-60560-375-9, Terre Haute, Indiana, May 2007

Summy, K.R., Little, C.R., Everitt, J.H., Mazariegos, R.A., French, J.V., Setamou, M., and Mata, J. (2010). Detection of incipient pest infestations on glasshouse crops using multispectral imagery and a common vegetation index. *Subtropical Plant Science*, Vol. 62, No. 1, pp. 56-62

Summy, K.R., Little, C.R., Mazariegos, R.A., Everitt, J.H., Davis, M.R., French, J.V., and Scott, A.W. (2003a). Detecting stress in glasshouse plants using color infrared imagery: a potential new application for remote sensing. *Subtropical Plant Science*, Vol. 55, No. 1, pp. 51-58

Summy, K.R., Little, C.R., Mazariegos, R.A., Everitt, J.H., Davis, M.R., French, J.V., and Scott, A.W. (2003b). Technical feasibility of color infrared imagery for monitoring physiological stress in glasshouse crops. *Proceedings of the 19th Biennial Workshop of Color Photography, Videography and Airborne Imaging for Resource Assessment*. ISBN 1-57083-074-6, Logan, Utah, October 2003

Summy, K.R., Little, C.R., Mazariegos, R.A., Hinojosa-Kettelkamp, D.L., Carter, J., Yousef, S., and Valdez, R. (2004). Evaluation of artificial lighting sources for the acquisition of color infrared imagery under glasshouse conditions. *Subtropical Plant Science*, Vol. 56, No. 1, pp. 44-51

Thomas, J.R., and Oerther, G.F. (1977). Estimation of crop conditions and sugar cane yields using photography. *American Society of Sugar Cane Proceedings*, Vol. 6, No. 1, pp. 93-99

Toler, R.W., Smith, D.B., and Harlan, J.C. (1981). Use of aerial color infrared photography to evaluate crop disease. *Plant Disease*, Vol. 75, No. 1 pp. 24-31

Wiegand, C.L., Gausman, H.W., Allen, W.A. (1972). Physiological factors and optical parameters as bases of vegetation discrimination and stress analysis. *Proceedings of the seminar on: Operational Remote Sensing Seminar*, Houston, Texas. American Society of Photogrammetry, Falls Church, Virginia, USA

Wilke, D.S., and Finn, J.T. (1996). Remote sensing imagery for natural resources monitoring. Columbia University Press, ISBN 0-23107-928-1, New York, New York, USA

Yepsen, R.B. (1984). *The encyclopedia of natural insect & disease control.* Rodale Press, ISBN 0-87857-488-3, Emmaus, Pennsylvania, USA

Yousef, S., Summy, K.R., and Little, C.R. (2011) Detection of salt toxicity and nitrogen deficiency in *Cucumis sativus* L. using spectroradiometry and color infrared imagery. *Journal of Plant Nutrition*, Vol. 34, No. 8, pp. 1236-1244